Concepts for morphing aerofoil sections using pantographic structures

N. M. Saeed & A. S. K. Kwan
Cardiff School of Engineering, Cardiff University, UK

Abstract

Morphing structures have great importance in numerous engineering applications, and have significant potential in the aerospace industry. An aircraft structure has different aerodynamic requirements for different stages of flight, and an optimal aircraft structure would also have different optimal shapes and geometry for these different requirements. A morphing structure has capability to provide for variable geometry. In this research, suitable morphing aerofoil structures have been found, as alternatives to the traditional aerofoil, and they provide larger lift (C_L) and smaller drag (C_D) coefficients. The morphing aerofoil structures proposed are achieved via series of interconnected, curved, single-actuator pantographs, with standard aerofoil NACA2415 chosen as the base-shape for comparative work. Two configurations have been studied in depth. The first consists of a small number of big pantographic elements, while the second consists of a large number of small pantograph elements. Results show that the second morphing structure exhibits a wider range of C_L and C_D than achievable by the first, and also by the standard NACA2415 with flaps. Taking the place of the traditional hinged control by the morphing aerofoil with smaller drag was shown to produce bigger lift. In addition, it was found that the morphing aerofoil can decrease the drag by more than 18%, especially in the starting stages of morphing. Furthermore, two useful and relatively simple methods have been presented in this paper, which provide a direct method for calculating required morphing shape displacements and calculating set of length actuations for bar assembly to adjust shape imperfection. This paper will cover the details of the geometry of the morphing structures and the aerodynamic properties of the different shapes during the morphing process.
Keywords: morphing structure, morphing aerofoil, NACA aerofoil, aerodynamic characteristics, shape adjustment.

WIT Transactions on The Built Environment, Vol 136, © 2014 WIT Press
www.witpress.com, ISSN 1743-3509 (on-line)
doi:10.2495/MAR140231

1 Introduction

Morphing structure is a type of structure which changes its shape according to its application. It has great importance in numerous engineering applications, especially in aerospace as arranging and controlling systems. Morphing structures increased the ability of engineers to improve designs of wing. The basic of inspiration of morphing structures is the natural world; e.g. a bird wing can take several different shapes for different flight requirements.

Initially, from the first successful flight by the Wright brothers, aircraft designers have been trying to progress the aircraft flight efficiency for different flying conditions, such as taking off, landing, for controlling flight attitude, rolling, pitching and yawing performance and for different weather condition. Since the shape of the aerofoil section is the principal and most responsive parameter for changing the flight characteristics of a wing, researchers working on "smart wings" have focused on finding different ways to change the flight efficiency and achieve the same aerodynamic effect in different flight conditions and environments.

Bliss and Bart-Smith [1] pointed out the feasibility for the morphing wing to be used to flight control. A morphing aerofoil technique by using complex composite cellular structures was invested by Bettini *et al.* [2]. Du and Ang [3] found that morphing aerofoil could replace the traditional hinged control aerofoil to control flight attitude with smaller drag and increased flight efficient.

Since some structures are very sensitive, for instance space structures could be distorted under loading or deployed in harsh environments, it is very necessary to restore or adjust such structures to the design/desired shape. This can be done by actuation of certain parameters, e.g. changing the length of a member. Work on the associated analytical/computational techniques is not extensive, and this is especially the case for direct approaches. Haftka and Adelman [4] studied shape control by thermal effects, and via placement of actuators (Haftka and Adelman [5]) with heuristic search. Such indirect approaches have also been tested by: Subramanian and Mohan [6] with an algorithm of successive correction based on heuristics. On the other hand, You [7] dealt with the problem directly and showed the direct link between length actuations and displacements for prestressed structures.

The purpose of this paper is to propose a morphing aerofoil to obtain a set of optimal aerofoil shapes to use instead of the traditional aerofoil with hinged flaps. The intention is to search for morphing structures that can perform as well as, or better than traditional aerofoils, in terms of lift coefficient (C_L) and drag coefficient (C_D). In addition, another purpose is to provide a direct relationship between bar length actuations and the nodal position/displacements in order to adjust joint displacement of the aerofoil as desired.

The outline of this paper is as follows. Some terminology and aerodynamic forces of aerofoil is briefly introduced in Section 2. Section 3 introduces the standard NACA2415 aerofoil. Sections 4 and 5 respectively deal with structure of proposed aerofoils and results of their performance as aerofoils. The technique of morphing shape calculation is illustrated in section 6. Section 7 transacts the

problem of finding a set of length actuation to achieve shape adjustments, and a concluding summary is presented in Section 8.

2 Terminology and aerodynamic forces of aerofoil

Aerofoil is a two dimensional cross-section shape of a wing, which is used to either generate lift or minimize drag when exposed to a moving fluid (Chandrala *et al.* [8]). Some of aerofoil terminologies are illustrated in Figure 1: The *mean camber line* is an imaginary curve on an aerofoil that divides it shortly into an upper half and lower half. The *Chord line* is an imaginary straight line connecting the leading edge of an aerofoil with its trailing edge. The *Camber* is the maximum distance between the mean camber line and the chord line, measured perpendicular to the chord line.

Leading Edge (LE) is the frontal point on the mean camber line while *trailing Edge (TE)* is the most backward point on the mean camber. The two important parameters governing aerofoil suitability are: the *Lift Coefficient* (C_L) which is a dimensionless coefficient that relates the lift generated by a lifting body, and it increases increasing by increasing camber and degree of angle of attack until stall; and the *Drag Coefficient* (C_D) which is a dimensionless coefficient presents the effective force produced by drag on an object. *Angle Of Attack (AOA)* is the angle between the chord line of an aerofoil and the relative wind and the *Flap Angle (FA)* is angle of the flaps, relative to the mean camber line, at the trailing edge of an aerofoil.

3 Standard NACA2415

For this work, the standard NACA2415 aerofoil is chosen as a comparator. This aerofoil is commonly used in light aircrafts, and is part of the Four-Digit Series (Leone and Teresi [9]). The first digit (2) represents the maximum camber in percentage of chord length while the second number (4) specifies the location of the maximum camber in tenths of chord length measured from leading edge. The last two digits (15) indicate the maximum thickness of the aerofoil in percentage of chord length.

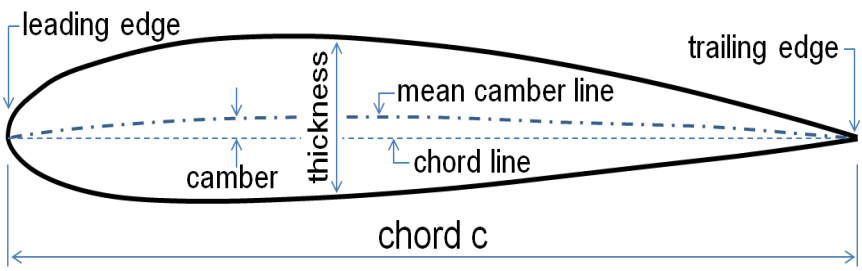

Figure 1: Aerofoil terminology.

4 Structure of proposed aerofoils

In this work, two shapes of morphing aerofoil are proposed. They are achieved via series of interconnected, curved, single-control pantographs. Aerofoil NACA2415 is chosen as the base-shape for constructing both proposed shapes. Configurations of the two morphing structures one (MAS1) and two (MAS2) are shown in Figures 2 and 3 respectively, with nine morphing stages to highlight the cross-sectional variation achieved through morphing. (Stages 2 and 8 are shown have been separately re-plotted with greater detail for each structure.) The first structure consists of a small number of big pantographic units while the second consists of high number of small pantographic units. Both aerofoil structures can provide the different shape configuration of camber, leading and trailing edge to fit flight environment and control the attitude. Both aerofoil structures are form by a main structure consists of series of interconnected, curved, single-control pantographs. Each pantographic unit is made from a pair of beams connected by a shear connector (which is central but typically not in the middle of the beams).

Each morphing structure also has a "control bar" (bar 36 in Figures 7 and 8) which is a bar of variable length that is used for controlling the shape configuration of the morphing aerofoil structure. The overall morphing pantograph mechanism has only one degree of freedom, so this control bar can be positioned in many different places, but only one is needed. In the experimental models in the current work, length actuation has been effected by a turnbuckle built into the control bar.

The morphing aerofoil is really the cross-sectional structure of the aerofoil, and hence a "stretchable skin" is also necessary to ensure correct aerodynamic properties (Du and Ang [3]). It may even be possible for such a "skin" to mimic the operation of wing feathers of a bird through overlapping plates.

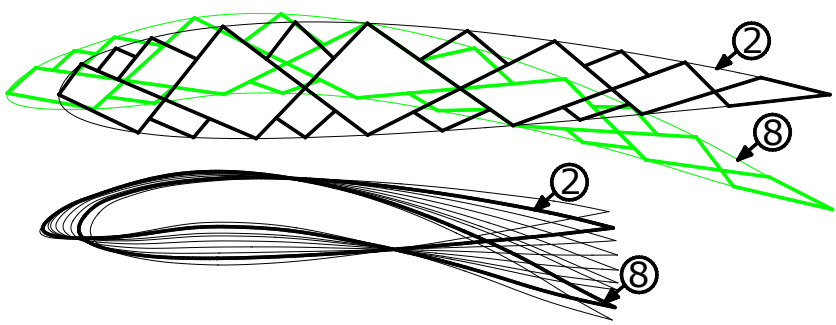

Figure 2: Nine morphing stages of proposed MAS1.

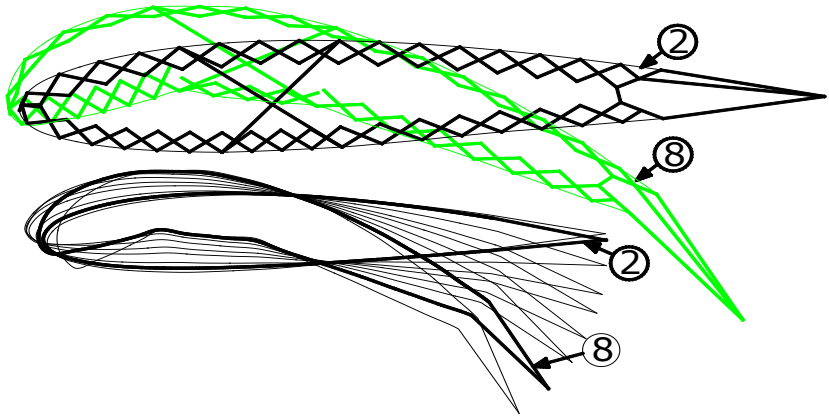

Figure 3: Nine morphing stages of proposed MAS2.

5 Results and discussion

For understanding the benefit of the proposed morphing aerofoil structures, it should be calculated and compared with the standard traditional hinged surface control aerofoil. The JavaFoil (v2.20) software was used for calculating Lift Coefficient (C_L) and Drag Coefficient (C_D) of the proposed and standard NACA aerofoils. Detailed coordinate of nine morphing stages for each morphing structure was carefully determined, and entered into JavaFoil. The changing sectional shapes cover leading edge, chamber, thickness, width and leading edge of aerofoil to suit different flight environment. Air speed of Mach 0.045 and Reynolds number 300000 were chosen for the calculations because these values have been used in the literature, and hence a verification of the JavaFoil calculations can be obtained.

5.1 Comparing C_L, C_D of the proposed aerofoils with NACA2415

C_L and C_D relationship of morphing aerofoil structure one (MAS1), morphing aerofoil structure two (MAS2) and standard NACA2415 are shown in Figure 4, where values are obtained by changing the angle of attack. These coefficients are calculated from the shape of the nine morphing stages of MAS1 and MAS2.

Figure 4 shows that in general both MAS1 and MAS2 provide less C_D as compared to NACA2415. In addition, both the maximum C_L of MAS1 and MAS2 are greater than the peak C_L achievable by NACA2415. The C_L versus C_D graph of MAS1 started from stage 1 with C_L rises rapidly until stage 5, and it rises more gradually thereafter until stage 9 which has maximum C_L and C_D. For MAS2, C_L becomes less and less dependent on C_D with increasing stages.

Figure 5 presents the comparison of C_L and C_D of MAS1 and MAS2 and standard NACA2415 achieved via increasing flap angles (with angle of attack remaining fixed). MAS2 and MAS1 exhibit a wider range of C_L and C_D than achievable by standard NACA2415 with flaps. Again, MAS2 shows a smooth

relationship throughout, but MAS1 displays a small step change around $C_D = 0.02$, which is likely to be caused by aerofoil surface not smooth enough. A similar step change, but more pronounced, is seen for the NACA aerofoil at around the same $C_D = 0.02$ zone, but the reason there is due to, certain angle of attack, the trailing edge of the aerofoil is suddenly no longer "hidden" behind maximum thickness, but appears behind the horizontal position of maximum thickness, thus causing additional drag.

In summary, it is found that the morphing aerofoil is more effective than NACA2415 for producing bigger C_L for the same amount of C_D.

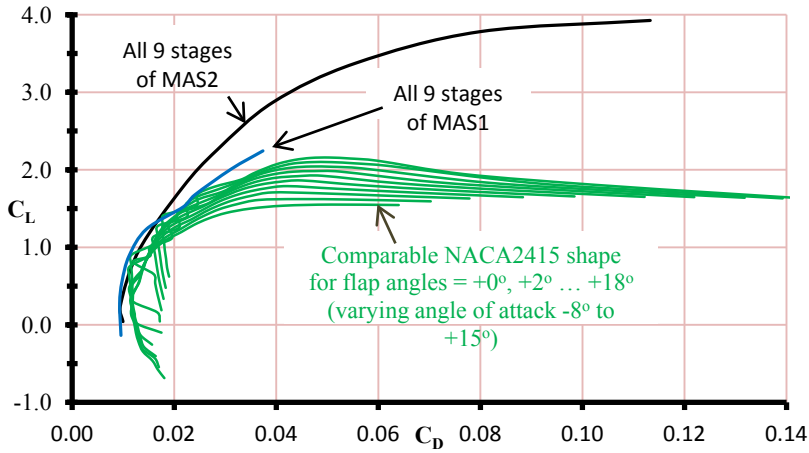

Figure 4: Comparing C_L, C_D of NACA2415 (fixing FA, varying AOA) with MAS1 and MAS2.

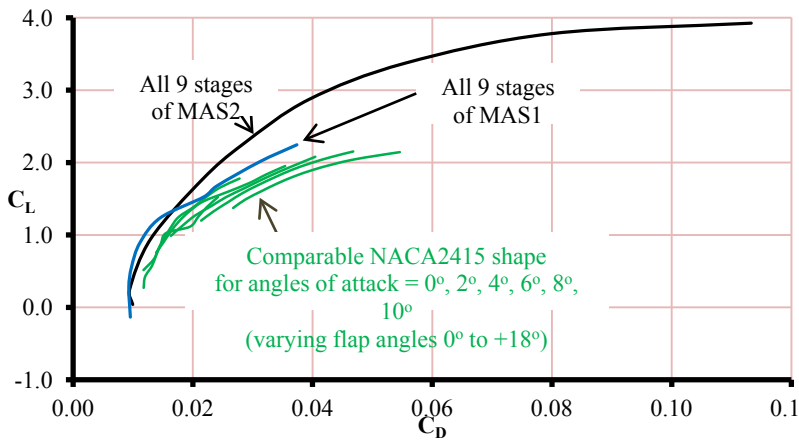

Figure 5: Comparing C_L, C_D of NACA2415 (fixing AOA, varying FA) with MAS1 and MAS2.

5.2 Comparing C_L, C_D of the proposed aerofoils with 31 NACA2415 shapes

Figure 6 shows a group of results of aerodynamic characteristics C_L and C_D relationship of MAS1 and MAS2 compared the 31 standard NACA shapes. The C_L and C_D of those 31 standard NACA shapes come via increasing angle of attack from -10° to +25°. MAS2 exhibits a wider range of C_L and C_D than achievable by the 31 NACA shapes, but MAS1 is in the inside of their range. Mostly, C_D of MAS1 and MAS2 is smaller than the 31 standard NACA shapes for the same C_L. In the zone of $C_L \approx 2.0$, C_D of MAS1 and MAS2 are greater than C_D of the shapes NACA6415 to NACA9420. The effect of having big camber leads to increase in C_L, which is followed by decrease the pressure drag due to the decrease of the cross sectional area, and thus a smaller C_D produced. Therefore, both MAS1 and MAS2 provide greater lift (for the same drag) than the whole NACA family of aerofoil shapes.

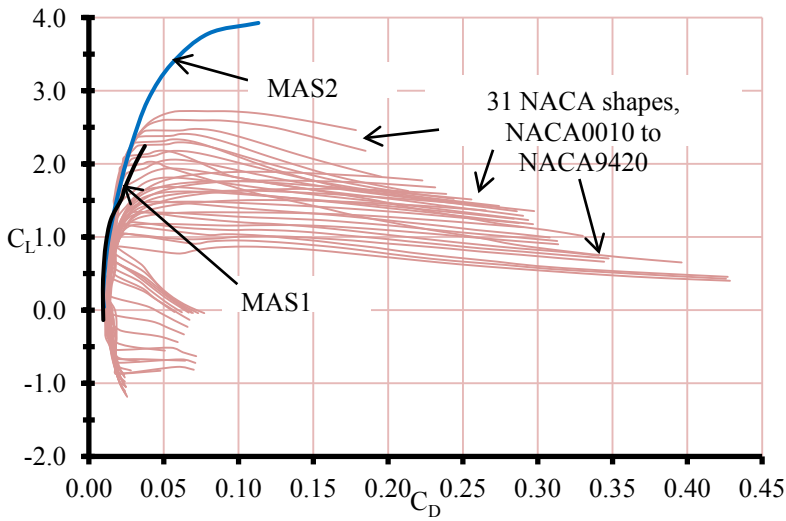

Figure 6: Comparing C_L, C_D of 31 NACA2415 shapes with MAS1 & MAS2.

6 Morphing deflection calculation

The comparison of experimental and analytical model is very important to prove the using of morphing structure for morphing aerofoil as an effective way to replace the tradition aerofoil. The deflection analysis due to the loading and actuation of morphing control bar can be calculated by Equation 1. Force method was used for calculation of total displacement of the required joints, which contains two types of displacements. The first is the vector of nodal displacements of the structure due only to load, and the second is the resultant nodal displacements after some bar elongation actuation e_o has been applied. The

combination of both deflections was done by superposition, and a Matlab programme was prepared for this work.

In this paper, an experimental has been done on a demonstration model of the morphing aerofoil shape structure and compared to the theoretical results linearly and non-linearly (coordinate update method). For instance the two joints (Joints 1 and 19) are selected which are the most frontal and most backward joints as shown in Figures 10 and 11 respectively. In this experiment, one effective bar (bar 36) is selected to provide different shapes of the structure.

$$d = B^{+}\ e\,. \tag{1}$$

where

$e = e_o + F\,(t_H + S\,\alpha)$

$\alpha = -(S^T F\, S)^{-1}\,[S^T e_o + S^T F\ t_H]$

$t_H = A^{+}\ p$

A^{+} and $B^{+}$is are the pseudo-inverse of equilibrium matrix A and B, F is the flexibility matrix, d is the external nodal displacements, e is the total internal bar elongation, e_o is the elongation actuation of each bar, p is the vector of external loads, S is the states of self-stress and equal to nullspace (A).

As shown in both Figures 7 and 8, generally the experimental results agree well with non-linear theoretical results though all the three curves (linear, non-linear and experiment) correlate closely to each other in the beginning stages of morphing. Horizontal displacement results agree better with theoretical predictions than the vertical displacements in both selected joints. Any difference between results could result from the shape of the physical being imperfect from construction, and the imperfections exacerbate the distortion from theoretical shape at the latter of morphing. For sorting such kind of problems, the techniques for structure adjustment become necessary, as briefly illustrated in the next section.

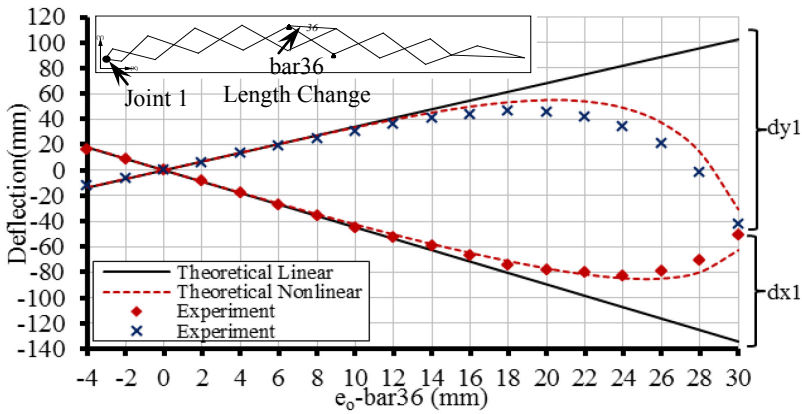

Figure 7: Theoretical and experimental deflection versus bar deflection of joint 1 in x and y direction.

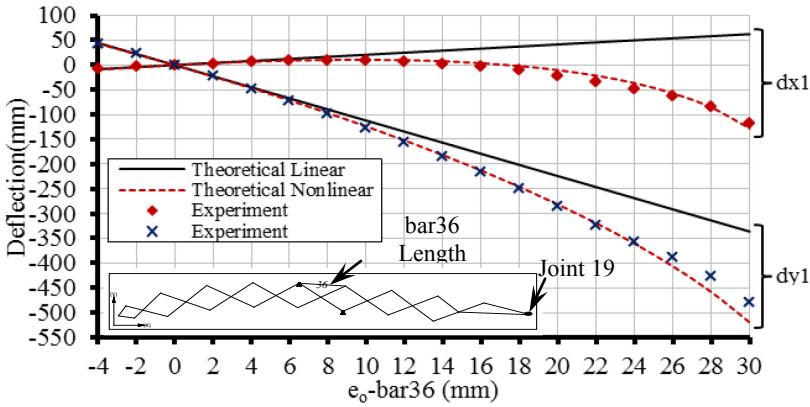

Figure 8: Theoretical and experimental deflection versus bar deflection of joint 19 in x and y direction.

7 Adjustment of imperfect shape

In this paper, focus has been on behaviour of proposed morphing aerofoil. From the comparison of morphing results, only small differences were noticed between theoretical desired shapes and the measured experimental shapes of a physical model of the pantograph morphing aerofoil. Sometimes the model not fit with the wanted shape due to manufacture or assembly imperfection, or due to environmental effects (*e.g.* thermal distortion) or the structure moving. For this purpose, the technique of structure shape adjustment was applied to restore the shape to the desired shape.

The process of shape adjustment of the structure is that a small nodal change the structure shape is achieved to correct the shape to a desired shape through applying length (or rotation) actuation to some bar, e.g. by using turnbuckles. The necessary information is simply the displacements of the outside joint of the morphing aerofoil to be controlled (*i.e.* not all the displacements) as they stand, and what values they should become. Equation 2 is the governing equation of this technique, and it specifically isolates the effects due to e_o from any other effects.

$$Y\, e_o = d_n - d_c \tag{2}$$

where $Y = B^+ - B^+ F S (S^T F S)^{-1} S^T$, d_c is vector of current displacements (due to whatever cause) and d_n is the new resultant displacements after the application of e_o.

Figure 9 illustrates the results of adjustment, which comes from modifying measured position of joints after morphing to the desired position through applying output set of $\mathbf{e_o}$ from the Matlab program of the Equation 2 to the structure model. As a rule, the results are good.

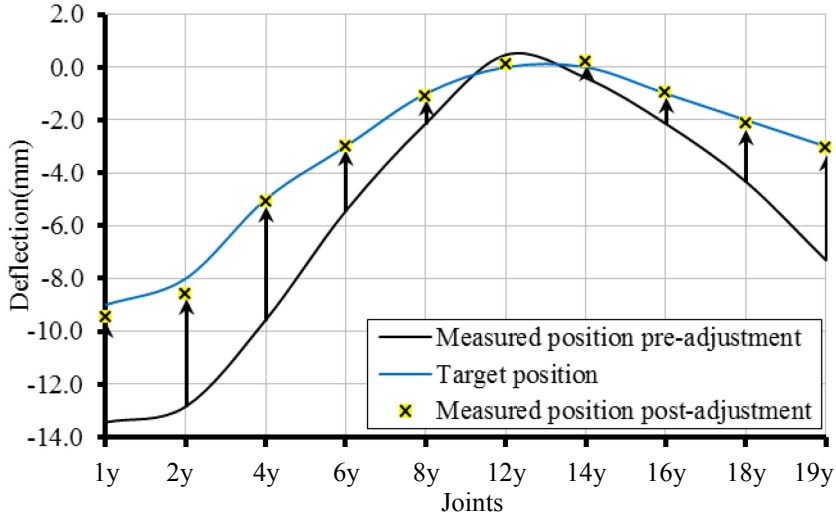

Figure 9: Adjustment of top joints in y-direction under loading

8 Conclusion

Two morphing aerofoils have been formed a series of interconnected curved controlled pantograph units. Morphing aerofoil structure 2 exhibits a wider range of C_L and C_D than achievable by morphing aerofoil structure 1 and standard NACA2415 with flaps. Taking the place of the traditional hinged control by the morphing aerofoil with smaller drag was proven for production of bigger lift.

Morphing aerofoil structure 1 can have 18% lower drag than average while drag of the morphing aerofoil structure 2 could be 19.5% lower than average in the starting stages of morphing. The maximum C_L value of morphing aerofoil structure was 2.5% higher than the C_L of the NACA2415 whereas for morphing aerofoil structure 2, the gain was 1.82 times.

In addition, two useful and relatively simple methods have been presented in this paper, which provides a direct method for calculating required morphing shape displacements and calculating set of length actuations for bar assembly to adjust shape imperfection.

References

[1] Bliss, T. K. & Bart-Smith, H., Morphing structures technology and its application to flight control, *In Proceedings of Student Research Conference*, Virginia Space Grant Consortium Newport News, Virginia, USA, 1 April 2005.

[2] Bettini, P., Airoldi, A., Sala, G., Landro, L. D., Ruzzene, M. & Spadoni, A., Composite chiral structures for morphing airfoils: numerical analyses and

development of a manufacturing process. *Composites Part B - Engineering*, 6(2), pp. 133-147, 2010.
[3] Du, S. & Ang, H., Design and Feasibility Analyses of Morphing Airfoil Used to Control Flight Attitude. *Journal of Mechanical Engineering*, 58(1), pp. 46-55, 2012.
[4] Haftka, R. T. & Adelman H. M., Analytical investigation of the static shape control of large space structures by applied temperature. AIAA Journal, 23(3), pp. 450-457, 1985a.
[5] Haftka, R. T. & Adelman, H. M., Selection of actuator locations for static shape control of large space structures by heuristic integer programming. *Computers and Structures*, 20(1-3), pp. 575-582, 1985b.
[6] Subramanian, G. & Mohan, P., A fast algorithm for the static shape control of flexible structures. *Computers and Structures*, 59(3), pp. 485-488, 1996.
[7] You, Z., Displacement control of prestressed structures. *Computer Methods in Applied Mechanics and Engineering*, 144(1-2), pp. 51-59, 1997.
[8] Chandrala, M., Choubey, A. & Gupta B., Aerodynamic Analysis Of Horizontal Axis Wind Turbine Blade. *International Journal of Engineering Research and Applications (IJERA)*, 2(6), pp. 1244-1248, 2012.
[9] Leone, A. & Teresi, L., Numerical study of aeroelasticity of sails. *COMSOL Users Conference*, Milano, 2006.